ACS Chemical Neuroscience

pubs.acs.org/chemneuro

Research Article

Single Molecule Fingerprinting Reveals Different Amplification Properties of α-Synuclein Oligomers and Preformed Fibrils in Seeding Assay

Derrick Lau, Chloé Magnan, Kathryn Hill, Antony Cooper,* Yann Gambin,* and Emma Sierecki*

Cite This: *ACS Chem. Neurosci.* 2022, 13, 883–896

Read Online

ACCESS | Metrics & More | Article Recommendations | Supporting Information

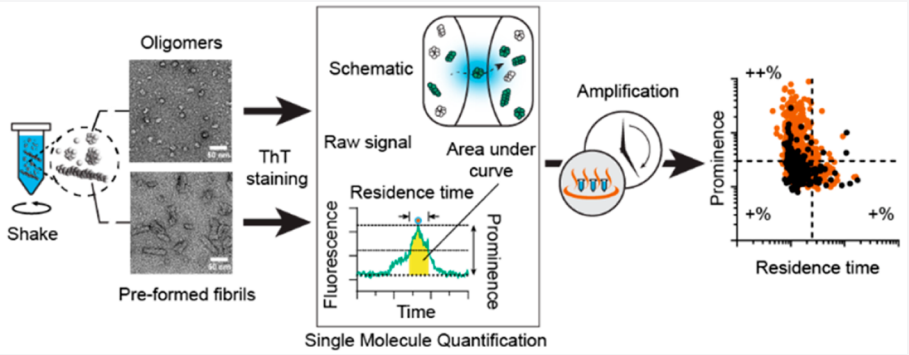

ABSTRACT: The quantification of α-synuclein aggregates has emerged as a promising biomarker for synucleinopathies. Assays that amplify and detect such aggregates have revealed the presence of seeding-competent species in biosamples of patients diagnosed with Parkinson's disease. However, multiple species, such as oligomers and amyloid fibrils, are formed during the aggregation of α-synuclein; these species are likely to coexist in biological samples, and thus it remains unclear which species(s) are contributing to the signal detected in seeding assays. To identify individual contributions to the amplification process, recombinant oligomers and preformed fibrils were produced and purified to characterize their individual biochemical and seeding potential. Here, we used single molecule spectroscopy to track the formation and purification of oligomers and fibrils at the single particle level and compare their respective seeding potential in an amplification assay. Single molecule detection validates that size-exclusion chromatography efficiently separates oligomers from fibrils. Oligomers were found to be seeding-competent, but our results reveal that their seeding behavior is very different compared to that of preformed fibrils, in our amplification assay. Overall, our data suggest that even a low number of preformed fibrils present in biosamples is likely to dominate the response in seeding assays.

KEYWORDS: *α-Synuclein, Parkinson's disease, single molecule detection, oligomers, preformed fibrils, seed amplification assay, real time quaking induced conversion, protein misfolding cyclic amplification assay, RT-QuIC, PMCA*

INTRODUCTION

Parkinson's disease (PD) is characterized by the loss of neurons within the *substantia nigra pars compacta*, resulting in motor symptoms of tremors and rigidity to limbs, bradykinesia, and stooped postures.[1] Although the etiology of PD is still not well understood, it is established that α-synuclein (α-syn) plays a central role in both idiopathic and familial forms of the disease. α-Syn is a 14 kDa synaptic protein found across many cells of the central nervous system and highly enriched in dopaminergic neurons.[2] Missense mutations of the α-syn encoding gene *SNCA* lead to an increased propensity of α-syn to aggregate into fibrils and are linked to familial forms of the disease.[3−5] Allele duplication of the *SNCA* gene also leads to PD.[6] It is hypothesized that α-syn aggregates are the catalysts that lead to the eventual formation of dense and compact intraneuronal inclusions known as Lewy bodies, the pathological hallmark of PD.[7] Dementia with Lewy bodies (DLB) and multiple system atrophy (MSA) are also clinically related to PD with the presence of intracellular α-syn aggregates. The consistent presence of α-syn aggregates in these pathologies and the demonstrated ability of these aggregates to spread to other cells with prion-like behavior make pathogenic forms of α-syn both a promising biomarker of synucleinopathies and a likely pathogenic mechanism of disease progression. Recent developments, such as real time quaking induced conversion

Received: August 18, 2021
Accepted: December 20, 2021
Published: March 14, 2022

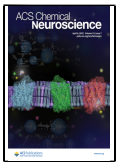

https://doi.org/10.1021/acschemneuro.1c00553
ACS Chem. Neurosci. 2022, 13, 883−896

(RT-QuIC) assay or protein misfolding cyclic amplification (PMCA) assay utilize the self-templated amplification of α-syn to detect the presence of α-syn aggregates in biofluids, in particular, cerebrospinal fluid (CSF). Using these seed amplification assays (SAAs), different groups have successfully identified patients with diverse synucleinopathies.[8−10] Importantly, recent studies suggest that SAAs could identify PD patients in the prodromal phase,[11] offering new hope to the community.

The further development of amplification methods and quantitative assays requires the use of well-defined standards that recapitulate the behavior of the biological samples. Such standards have been difficult to identify when working with α-syn. For example, α-syn aggregates isolated from brains encompass a range of post-translational modifications, including truncations,[12,13] phosphorylation,[14] acetylation,[12] nitration,[15] and ubiquitination.[16] These modified α-syn aggregates are too heterogeneous to become reliable standards. Preformed aggregates generated from recombinant proteins have been utilized, but even this material can be difficult to standardize between laboratories.[4,17−20] One object of debate in using preformed aggregates has been the relevance of using α-syn fibrils compared to oligomers. Indeed, during the self-association process, both *in vitro* and *in vivo*, α-syn is thought to change from a mainly unstructured monomer to form small, soluble oligomers (consisting of 30−50 monomers). A structural switch to antiparallel β-sheet is required for the oligomers[21] to form protofibrils that can "grow" by recruiting and incorporating more α-syn monomers, generating long amyloid fibrils. The pathological relevance of α-syn oligomers and fibrils remains undecided. α-Syn oligomers appear to be the more toxic species, at least in the short term, as they have been shown to bind and disrupt cellular membranes and participate in mitochondrial and lysosomal dysfunction.[4,22−25] Oligomers also affect proteasome activity[26] and vesicular trafficking or induce endoplasmic reticulum stress by toxic gain-of-function changes.[27] Furthermore, α-syn fibrils constitute the majority of Lewy bodies and participate in the sequestration of important cellular factors such as mitochondria,[28] driving cell dysfunction and cell death. Early products from the aggregation process are partially reversible, and α-syn fibrils could serve as a reservoir of oligomers.[29,30] Because of the difference in biological activity, the question of whether oligomers or fibrils are the most relevant species to serve as biomarkers arose. The high sensitivity of the seed amplification assays, in the low femtomolar range, makes this question more pressing, as even a minority species present in minute quantities could dominate the amplification outcome.

Here we use a newly developed single molecule fluorescence method to determine the "fingerprints" of α-syn oligomers and fibrils and assess their seeding potential in an amplification assay. Single molecule imaging is emerging as a powerful tool to study molecular dynamics with the ability to resolve microscopic events that are otherwise hidden in ensemble average measurements (see review by Priest et al.[31]). In this study, we profiled α-syn aggregates as they diffuse freely in solution using a 3D printed confocal microscope.[32] This plug-and-play device is designed to detect single aggregates labeled with the established fluorescent dye thioflavin T (ThT). When ThT reactive species cross the small excitation/detection confocal volume (~1 fL), individual peaks of fluorescence are detected above background. In addition to counting aggregates, this method also determines the ThT reactivity (prominence) and apparent size (residence time) for each event. We used this fingerprinting approach to track the formation and purification of oligomers that are currently evaluated as standards for seed amplification assays.[17,19] Our single molecule measurements revealed the rapid formation of oligomers and fibrils within 5 h of a standard aggregation reaction and demonstrated that size exclusion chromatography (SEC) was necessary to completely separate monomeric, oligomeric, and fibrillar species of α-syn. We then compared purified α-syn oligomers to sonicated α-syn fibrils, before and after an isothermal incubation with α-syn monomers to assess their amplification potentials. Our single molecule data show very different amplification profiles and seeding propensity for purified oligomers and fibrils. Our results suggest that in heterogeneous samples, a positive response in SAA would be mainly driven by the presence of fibrils.

RESULTS AND DISCUSSION

Principle of Single Molecule Profiling of α-Syn Aggregates. We and others have previously demonstrated that single molecule fluorescence assays were compatible with the use of thioflavin T (ThT) to observe and characterize human α-syn oligomers and larger soluble aggregates (Figure 1A).[8,33,34] We have shown that single molecule detection enables a >100000-fold increase in sensitivity over traditional plate reader measurements for ThT.[32] Traditionally, single

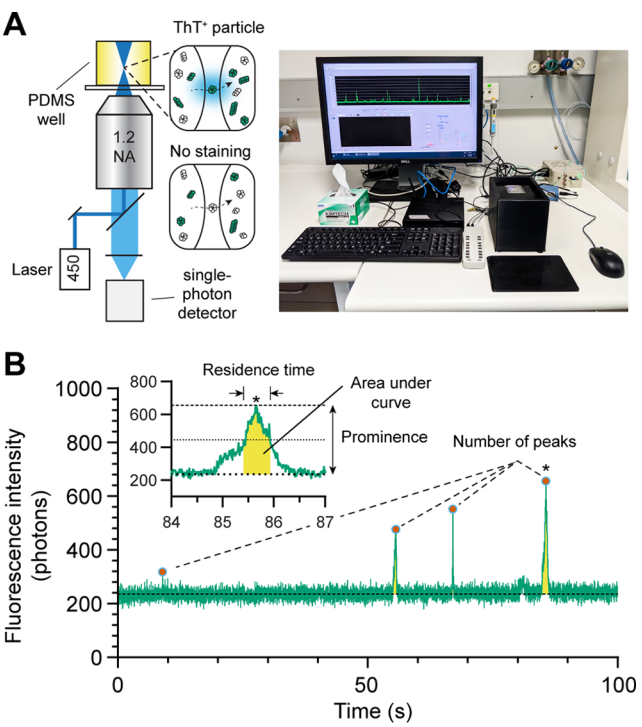

Figure 1. Single molecule fingerprinting for the characterization of α-synuclein species. (A) (left) Schematic of the microscope setup. The inset shows ThT stained and unstained (dark) α-syn oligomers or fibrils (green and white colored particles) diffusing across the confocal volume. Monomeric α-syn and some assemblies do not bind ThT. (right) Photograph of the microscope for recording the fluorescence traces. (B) Characterization of fluorescence traces. A fluorescence trace is analyzed to report the total number of peaks (events) and the prominence of individual peaks, residence time (full width half-maximum), and area under the curve (yellow). The inset shows a region denoted by (*) in the trace.

https://doi.org/10.1021/acschemneuro.1c00553
ACS Chem. Neurosci. 2022, 13, 883−896

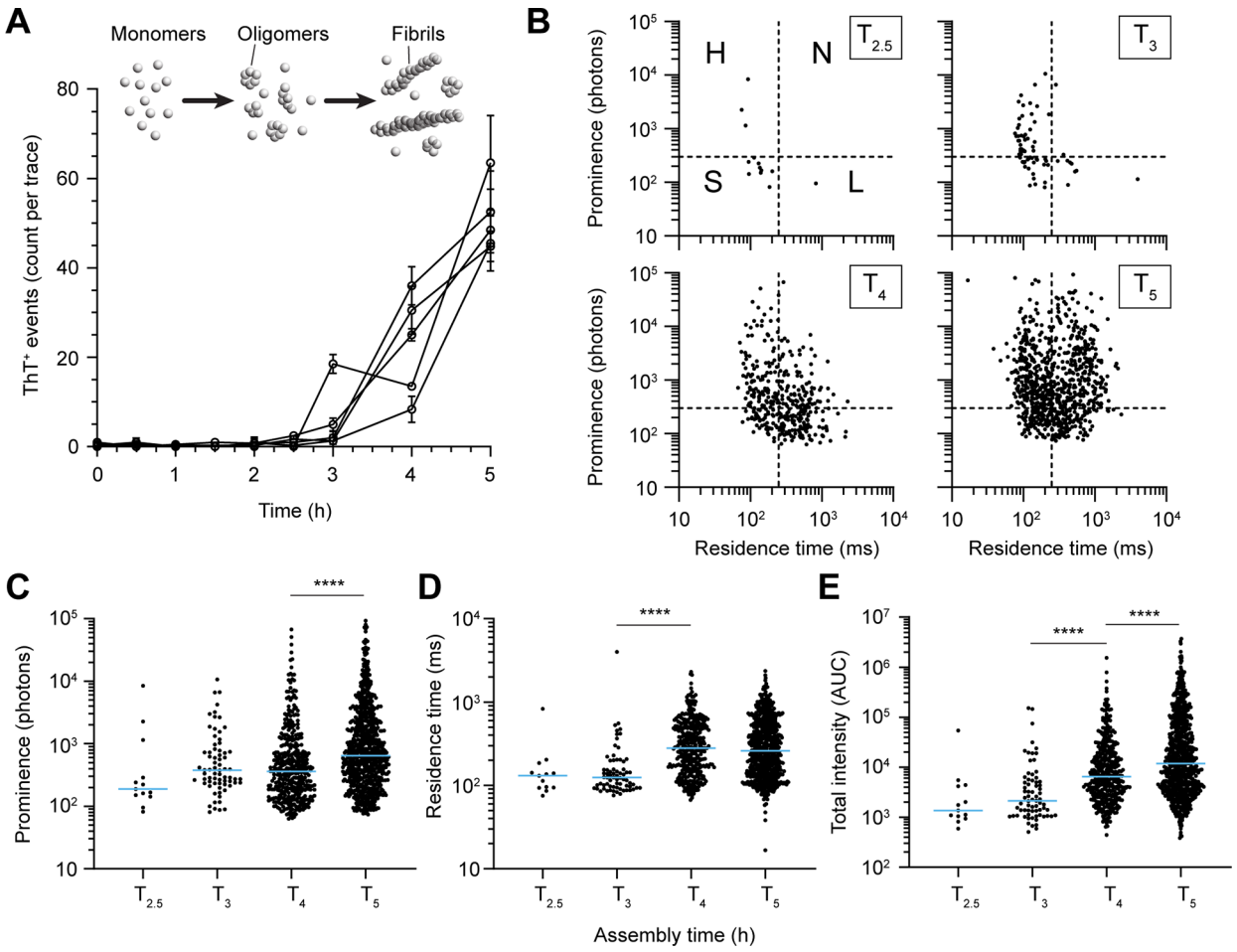

Figure 2. Single molecule aggregation kinetics and fingerprinting of species. (A) Number of ThT$^+$ species detected during the time course of α-syn aggregation. Each curve corresponds to an independent aggregation experiment. Error bars represent the standard deviation. (B) Single molecule fingerprinting of ThT$^+$ peaks detected. Peak prominence is plotted against residence time from 2.5 h. Four types of particles can be defined: small (S), high (H), long (L), and neutral (N). The cut-offs were set at 250 ms and 300 photons, on the x- and y-axis, respectively. (C−E) Scatter plots comparing prominence (C), residence time (D), and total intensity (E). Blue line represents the median values. Each symbol represents an individual peak detected in the fluorescence traces generated from five independent experiments in panel A. Statistics used Kruskal−Wallis one-way ANOVA, $p \leq 0.0001$ (****).

molecule measurements are performed on expensive commercial microscopes or on homemade setups that are difficult to replicate between laboratories. To improve access to this method, we designed a small device ("AttoBright") to perform counting and characterization of single aggregates; the device can be easily replicated by 3D plastic printing.[32] ThT-stained (ThT$^+$) particles are detected on this AttoBright microscope as they diffuse across the confocal volume, producing large bursts of fluorescent intensity (event) in the trace (Figure 1A). α-Syn aggregates containing β-sheets bind strongly to ThT, while monomeric α-syn does not bind to ThT. Fluorescence traces can then be quantitatively analyzed using an automated algorithm to report the number of ThT$^+$ events per trace, as well as the prominence (burst intensity), residence time, and total intensity (i.e., the sum of all intensities to calculate the area under the curve) of each event (Figure 1B). The prominence and total intensity report on the number of ThT molecules bound per particle, while the residence time, extracted using the full width at half-maximum (fwhm, time difference taken at half prominence), shows changes in size or compactness of ThT-labeled α-syn aggregates. Overall, the algorithm designed here can extract biophysical properties of individual α-syn aggregates to generate a profile or fingerprint of α-syn subspecies in the population.

Rapid Kinetics and Heterogeneity in the Early Aggregation Process. The AttoBright's ability to detect and characterize α-syn aggregates at single molecule level provided the opportunity to examine the early molecular events of aggregation. Monomeric α-syn was incubated with shaking to produce oligomers.[17] Aliquots were taken at different time points during the reaction and diluted for single molecule fingerprinting experiments. Individual ThT$^+$ peaks were detected as early as 2.5 h into the experiment (Supporting Figure 1). The number of events subsequently increased exponentially over time, generating a heterogeneous population of ThT$^+$ particles up to a maximum of 71 events per 100 s trace after 5 h (Figure 2A,B). The short lag phase observed here is reasonable given the high starting concentration of α-syn (12 mg/mL), which would increase the probability of primary nucleation.

The prominence of each event was plotted against its respective residence time to examine population heterogeneity and provide a single-molecule profile (fingerprint) of the sample, as previously described.[34] Briefly, ThT$^+$ particles were

https://doi.org/10.1021/acschemneuro.1c00553
ACS Chem. Neurosci. 2022, 13, 883−896

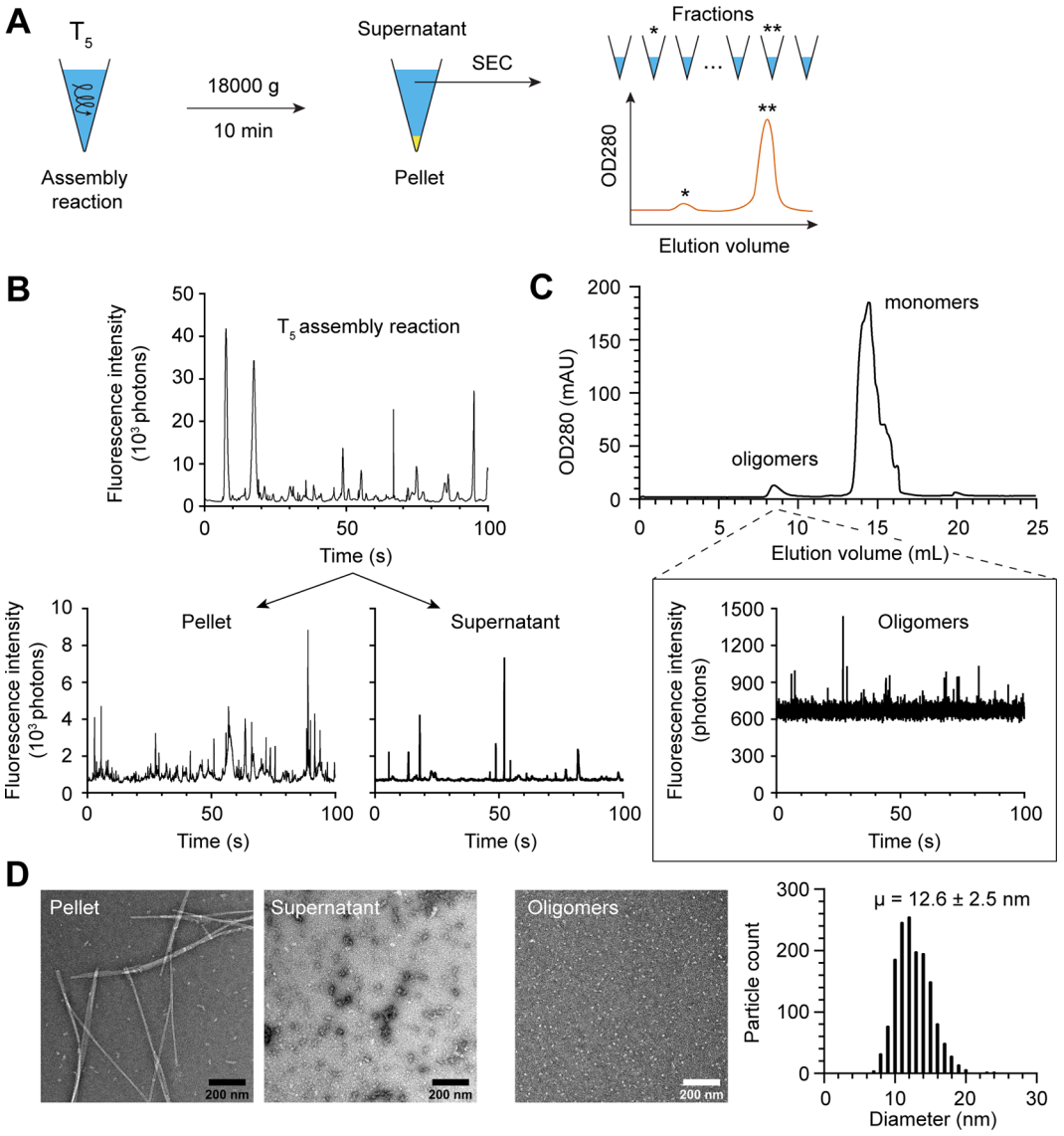

Figure 3. Isolation of α-syn oligomers. (A) Schematic of the experimental protocol to isolate and detect ThT^+ α-syn oligomers. After 5 h of aggregation, the reaction sample was centrifuged. The supernatant was further purified using size exclusion chromatography. Collected fractions were supplemented with monomers for amplification reactions and single molecule detection with ThT. (B) Representative fluorescence traces of supernatant and pellet fraction with corresponding electron micrographs of each fraction shown in panel D. (C) Gel filtration chromatogram identifying the elution peaks containing α-syn oligomers and monomers. A representative fluorescence trace corresponding to a fraction containing oligomers is shown. (D) Electron micrographs of the pellet, supernatant, and a SEC fraction containing oligomers. Scale bar is 200 nm. Histogram plot of the diameters of negatively stained particles from the [9.2−9.7 mL] SEC fraction; 12.6 ± 2.5 nm; 1544/2 (mean ± standard deviation; number of particles/fractions stained).

classed based on their distribution in each quadrant (Figure 2B) where events were defined as small (S, low prominence, short residence time), high (H, high prominence, short residence time), long (L, low prominence, long residence time), or neutral (N, high prominence, long residence time) with thresholds set at 300 photons and 250 ms, respectively. Our data showed that S type particles were the first to be synthesized during the *in vitro* oligomer-inducing protocol. A total of 13 particles, pooled from 5 experiments, were recorded at 2.5 h. These species likely represent small α-syn oligomeric aggregates and are characterized by a median prominence of 188 photons and median residence time of 130 ms (Figure 2C). The scatter profile showed significantly more particles after a further 30 min incubation and revealed the emergence of H type particles, from the possible conversion of S type oligomers. Interestingly, a small increase in prominence was noted with no change in the residence time (Figure 2B−D), possibly due to a conformational or structural change that increases ThT binding or fluorescence. Beyond 3 h incubation, we observed the appearance of higher order assemblies of N and L type (Supporting Figures 1 and 2) corresponding to larger particles with variable bound ThT ratios.

As expected, the total intensity increased over time (Figure 2E). Interestingly, our analysis shows a multistep assembly process. The first ThT^+ species at early time points (<3 h) are fast-diffusing, but after 3 h, their residence time increased significantly (median of 124 to 281 ms, Figure 2D) while their prominence remained unchanged (median 378 to 360 photons, Figure 2C). In the following step, a significant change in prominence became the main contributor to total

https://doi.org/10.1021/acschemneuro.1c00553
ACS Chem. Neurosci. 2022, 13, 883−896

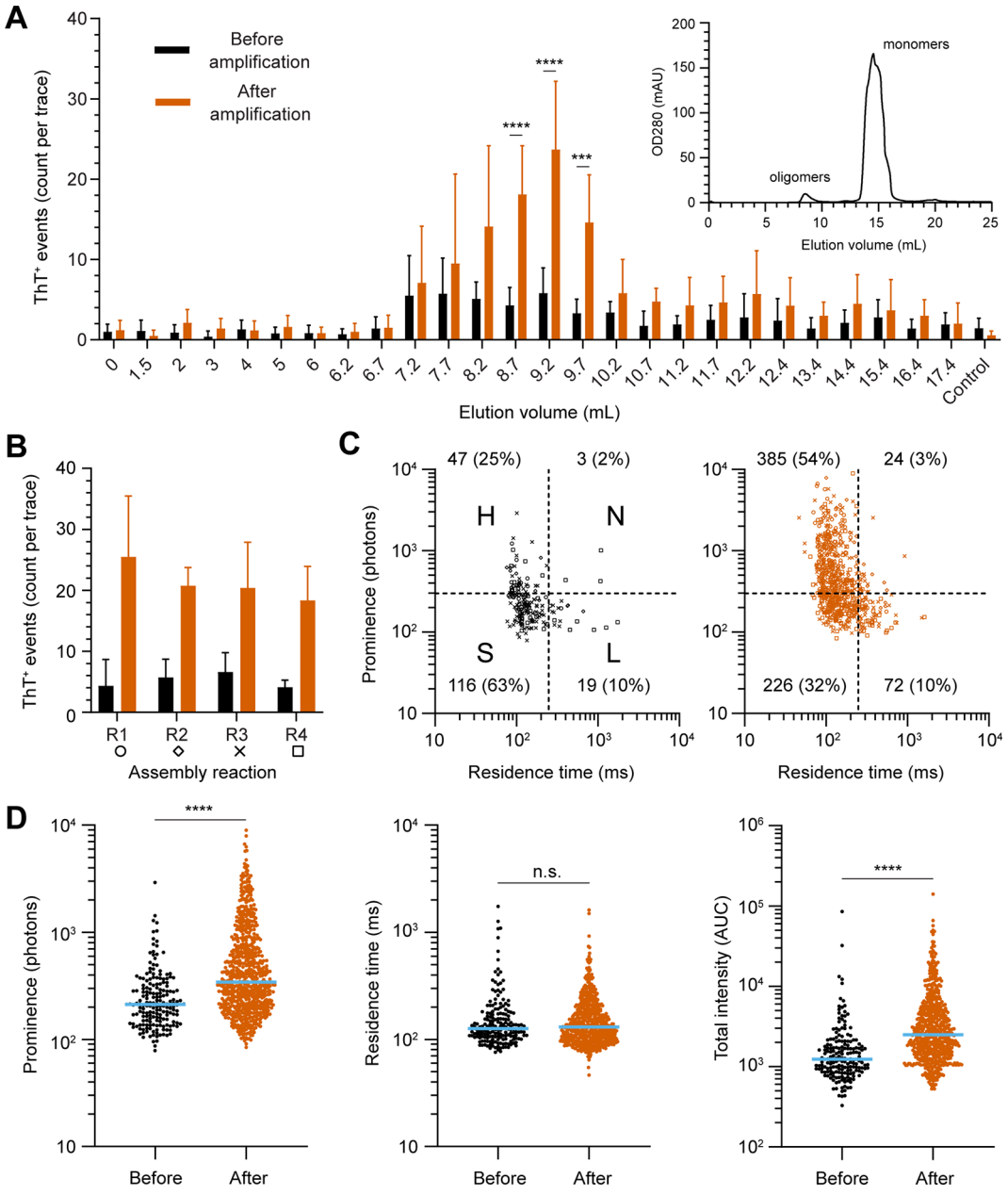

Figure 4. Single molecule characterization of α-syn oligomers. (A) Quantification of ThT$^+$ events detected in each fraction after size exclusion, before (black) and after an amplification step (red) in PBS. Negative control is monomeric α-syn and ThT in PBS. A gel filtration profile is shown in the inset for reference. Error bars represent the standard deviation. This color scheme is applied across all figures in this study. (B) Bar graph of the number of ThT$^+$ events detected in fractions containing oligomers (elution volume 7.7−10.2 mL) collected from four assembly reactions (R1−R4). (C) Single molecule fingerprinting of oligomers, before (left) and after amplification (right), is obtained by plotting the prominence against residence time. Each symbol represents an individual event with the shape corresponding to R1−R4 coded in panel B. Quadrant numbers report the number of particles in each quadrant and abundance. (D) Logarithmic scatter plot comparing peak prominence, residence time, and area under the curve before and after amplification. Each symbol represents an individual event (N = 34/34 traces before/after amplification). The median value is highlighted in blue. Statistics used Mann−Whitney t test, $p \leq 0.0001$ (****), nonsignificant (n.s.).

intensity increase, at 4−5 h. The L and N particles likely correspond to fibrils and fibrillar aggregates, respectively, and this was eventually verified by transmission electron microscopy (Figure 3). We were unable to assert whether L and N particles were produced from the direct conversion of S or H particles or both.

Overall, these observations agreed with the α-syn nucleation cascade hypothesis that aggregation is a stepwise process driven by conversion of monomeric α-syn to small seeds (S-type) that will catalyze the formation of more ThT reactive particles (H-type), possibly protofilaments, eventually forming fibrils and fibrillar aggregates (L- or N-type).[21,35,36] Importantly, these data demonstrate that *in vitro* synthesis generates a heterogeneous population of particles in the early aggregation process. Specifically, we show that a significant number of fibrils are produced within the first 5 h. These data emphasize the importance of performing additional steps to remove fibrils if a study makes explicit use of α-syn oligomers only.

Next, we were interested in isolating the oligomeric species, to compare their seeding potential with fibrils. To do so, we

https://doi.org/10.1021/acschemneuro.1c00553
ACS Chem. Neurosci. 2022, 13, 883−896

first removed the large fibrils and aggregates by centrifugation, followed by size-exclusion chromatography using the two-step purification protocol prescribed by Kumar et al.[17] (Figure 3A).

Removal of α-Syn Fibrils Is Incomplete by Low-Speed Centrifugation. We centrifuged the 5 h reaction mixture at high speed (18000*g*, 10 min) to separate fibrils and smaller oligomers or aggregates. This centrifugal speed was slightly higher than the 12000*g* prescribed by Kumar et al.[17] As expected, single molecule fingerprinting of the pellet showed slow diffusing ThT$^+$ species (broad, high intensity events), in agreement with the presence of large fibrils observed under EM (Figure 3). Single molecule analysis of this low-speed supernatant shows the presence of bright particles (Figure 3B) and revealed a significant population of slow diffusing species, large aggregates or small fibrils (Supporting Figure 2). EM showed a heterogeneous population of small protofibrils and oligomers (Figure 3D). This observation is consistent with the suggestion by Kumar et al.[17] to use SEC to further purify the small oligomers.

Coupling Single Molecule Detection on Size Exclusion Chromatography Demonstrates That Isolation of α-Syn Oligomers Is Efficient and Highly Reproducible. Next, we coupled our single molecule detection system with size exclusion chromatography to visualize the isolation of oligomers and validate that all residual fibrils were removed. To do this, we simply collected all eluted fractions and characterized the number and size of aggregates by single molecule fingerprinting. The SEC chromatogram revealed two elution peaks, at 8.5 and 14.5 mL, corresponding to oligomers and monomers in agreement with what has previously been reported (Figure 3C).[17,18,37] As shown in Figure 4A, we identified a cluster of ThT$^+$ events averaging 5.5 events per trace at the first elution peak in the SEC chromatogram, which corresponds to α-syn oligomers, according to previous publications.[17] In contrast, the low number of ThT$^+$ species in the α-syn monomers peak (14−16 mL) was comparable to background level, confirming that α-syn monomers were, as expected, not ThT reactive. Surprisingly, we did not detect the slower diffusing fibrillar ThT$^+$ species that were originally present in the supernatant in any eluted fractions (compare Figure 3B,C). We ascribed this discrepancy either to the poor stability of α-syn protofibrils and oligomers[29,37] with the dilution effect of gel filtration facilitating their disassembly[30] or to the loss of these fibrils due to sticking to the column matrix. Chromatograms obtained from four separate experiments showed identical profiles, demonstrating robust reproducibility.

EM observation of the 8.5 mL fraction (center of the oligomers peak) revealed particles with a narrow distribution of 12.6 ± 2.5 nm diameter (Figure 3D). The ultrastructure and dimension of these particles is within range of previous measurements of 12 nm.[17] Our single molecule fingerprinting reveals that only a fraction of the oligomers appears as ThT$^+$ species and that their profiles correspond exclusively to S- and H-type particles. Indeed, based on the concentration, not all of the α-syn oligomers are ThT reactive, and we later demonstrate the appearance of more ThT$^+$ species upon amplification. In conclusion, gel filtration is a valid and very reproducible approach for isolating α-syn oligomers (categorized as S and H fingerprints) as identical elution profiles were observed across purification of different batches of α-syn aggregation experiment.

Kumar et al. have also suggested the use of higher centrifugation (100000*g* for 30 min) to remove α-syn fibrils and simplify the isolation of oligomeric species. We collected the supernatant of reactions after this high-speed centrifugation and analyzed them by single molecule analysis. As expected, this supernatant presents significantly fewer N and L particles. However, our analysis reveals that the distribution of ThT$^+$ species is quite different from that of the SEC-purified fraction: the high-speed supernatant presents a larger number of aggregates with high ThT reactivity (species H, Supporting Figure 3). The profile of these peaks resembles the ones found in sonicated PFFs (see Figure 5B,C). One interpretation is that these species represent protofilaments or small protofibrils rather than oligomers, and we chose to focus on SEC-purified oligomers to assess their seeding potential.

Amplification Potential of α-Syn Oligomers. We speculated that oligomers isolated in the early steps of the

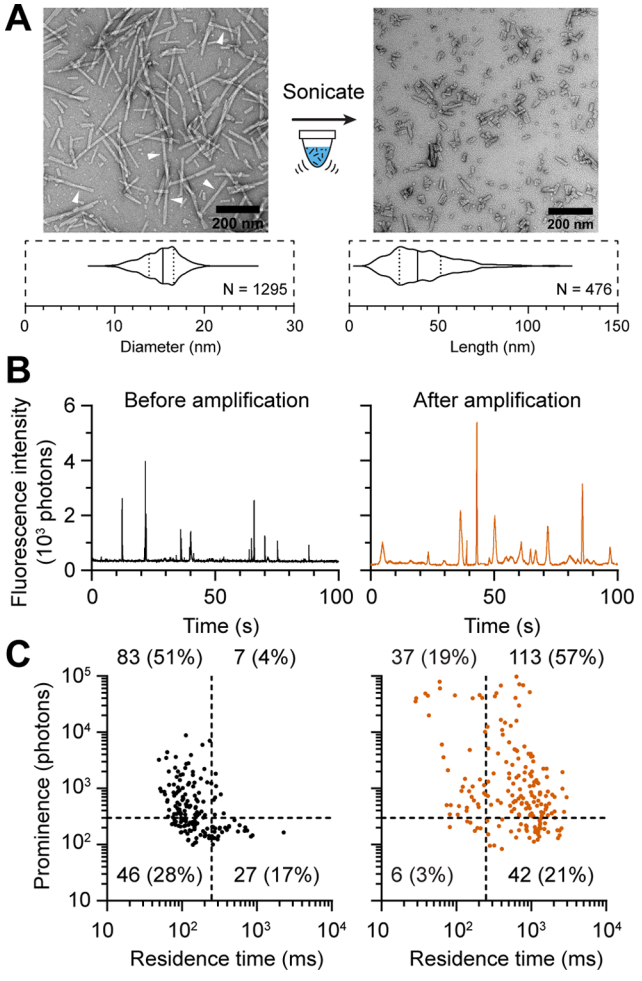

Figure 5. Single molecule fingerprinting of sonicated α-syn fibrils. (A) Negatively stained EM images of human α-syn fibrils before and after sonication. White arrows point at filamentous twists. Violin plot of tubular diameters of the fibrils prior to sonication and length of fibrils after sonication. Scale bar is 200 nm. (B) Representative fluorescence traces of sonicated fibrils before (black) and after a 5 h amplification (red). (C) Single molecule fingerprinting of sonicated mature human α-syn fibrils before and after amplification (red). Each symbol represents an individual event in the fluorescence traces. Quadrant numbers represent the number of ThT$^+$ events. Data are from three independent experiments.

https://doi.org/10.1021/acschemneuro.1c00553
ACS Chem. Neurosci. 2022, 13, 883−896

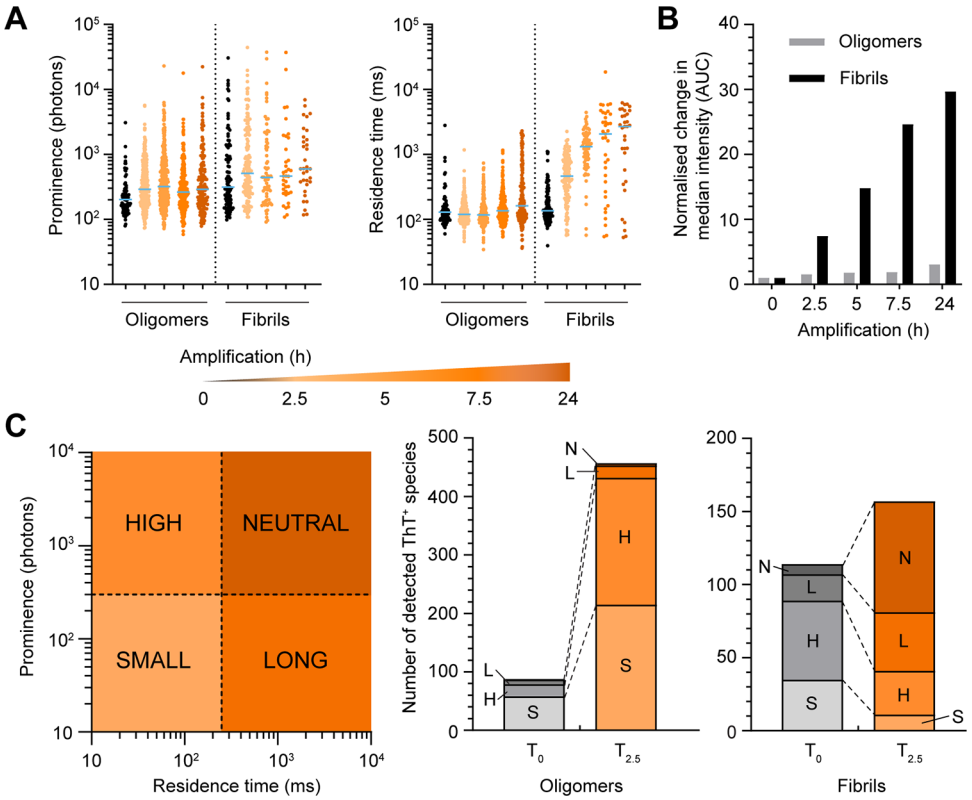

Figure 6. Time course amplification assay comparing α-syn oligomers and sonicated preformed fibrils. (A) Time course measurements of oligomers or fibrils amplified for 2.5, 5, 7.5, and 24 h (orange to red) in the presence of excess α-syn monomers and ThT in PBS. Scatter dot plots comparing the prominence and residence time. Each symbol represents an individual ThT$^+$ event. Data were collected from two independent experiments. The median value is highlighted in blue. (B) Bar graphs comparing the fold-change in median AUC of fibrils and oligomers of panel A. Value were normalized to the median total intensity collected at time 0. (C) Time comparison of the number of ThT$^+$ species of panel A detected from seeding experiment using α-syn oligomers or sonicated PFFs before and after 2.5 h incubation. Each type of ThT$^+$ species is coded by different shades of red.

aggregation process would be seeding competent given that they are hypothesized to be aggregation intermediates. To test this, we used an amplification assay where we added monomeric α-syn to all the SEC fractions and measured changes in ThT fluorescence after amplification. In this assay adapted for sensitive single molecule detection in small volumes, we use a single incubation step at 55 °C in nonshaking conditions and measure the same sample 5 h later (Supporting Figure 4).[34] We observed that amplification greatly enhanced the number of ThT$^+$ species in purified oligomers. Incubation at 37 °C produced a similar increase in ThT$^+$ species when seeded with oligomers (Supporting Figure 5). As shown in Figure 4A, the increase in ThT$^+$ reactivity was strictly limited to fractions containing α-syn oligomers ($p < 0.002$). In contrast, negative controls and monomeric α-syn displayed insignificant changes in ThT$^+$ species. Amplification of the oligomeric fractions obtained from 4 independent chromatographic runs (R1−R4) showed that the number of events consistently increased by at least 3 times in the oligomeric fractions (Figure 4B). Before amplification, single molecule profiling of these pooled particles showed that S-type particles (low prominence, low residence time) were the dominant species (63%, Figure 4C) followed by H type aggregates (25%). Importantly, large α-syn oligomers (>250 ms residence time, 12%) were in low abundance.

The increase in the number of S-type oligomers after the amplification step indicated the existence of dark (i.e., non-ThT reactive or has insufficient number of bound ThT molecules to overcome the background noise) seeding competent oligomers (Figure 4C). The absence or insignificant increase in ThT$^+$ events detected post-amplification in the negative control (30 μM α-syn monomers) and in SEC fractions containing α-syn monomers (EV ≈ 15 mL, Figure 4A) further indicate that these new S particles do not arise from *de novo* oligomerization. Concomitantly, we also observed an increase in the number of H particles (47 to 385), which represented the dominant species after amplification, while the N and L populations remained unchanged. The isolated oligomers therefore amplified with a distinctive pattern where the increase in total intensity (peak area) was only contributed by an increase in ThT reactivity with limited change in residence time (Figure 4D). The molecular signature of early oligomeric species can thus be best described by an upward transition from S to H particles (Figure 4C).

The Amplification Profile of α-Syn Is Distinct between Sonicated Fibrils and Oligomers. Next, we sought to characterize the amplification profile of α-syn PFFs and compare it with that of amplified α-syn oligomers to discern if they have a distinct *in vitro* signature. PFFs were created *in vitro* as described,[32] producing fibrils of 15.2 ± 2.1 nm in diameter (mean ± SD, Figure 5A) with longitudinal twists. This diameter is consistent with the "high salt strain" reported by Bousset et al.[38] To reduce the length of each fibril and make them amenable to spectroscopy measurement, PFFs were sonicated into smaller objects ranging from 10 to 120 nm (Figure 5A). Fluorescence measurement identified these

https://doi.org/10.1021/acschemneuro.1c00553
ACS Chem. Neurosci. 2022, 13, 883−896

particles as fast diffusing objects (<250 ms) with variable ThT reactivity (Figure 5B). Approximately 51% of these particles were H species with a maximum prominence of about 1 log larger compared to that of oligomers (Figure 5C). In the absence of heating (i.e., unamplified), the sonicated PFFs diffuse rapidly and their single molecule profile does not contain L and N particles. The residence times measured for sonicated PFFs and oligomers are relatively similar. This is not unexpected as for small rod-like fibrils, the diffusion time increases slowly as the fibril elongates (as predicted by hydrodynamic equations, see Supporting Information and Supporting Figure 6). Overall, sonicated PFFs with lengths up to 50 nm would only diffuse ~2-fold slower than oligomers. In contrast, a 5 h amplification of sonicated PFFs produced a significant right-ward lateral shift (longer residence time) in the profile where L and N particles became predominant, accounting for 78% of the detected species. This lateral shift in the profile was not attributed to heat induced aggregation or sonicated PFF seeds rejoining as only incubation in the presence of α-syn monomers produces this profile (see Supporting Results and Supporting Figure 7). This molecular fingerprint contrasts strongly with the amplification signature of α-syn oligomers that was previously characterized as an upward shift in ThT reactivity with little change in residence time.

We expanded our analysis by performing amplification kinetics to examine the evolution of species over time in seeded experiments. In longitudinal analysis, we noted that, again, the increase in total fluorescence upon α-syn oligomer seeding occurs through an increase in ThT reactivity with little change in residence time over the course of 24 h (Figure 6A). In contrast, the incubation of sonicated PFFs promoted rapid elongation of fibrils as evident from the 3-fold increase in median residence time after 2.5 h of incubation. Incubation of 2.5 h was sufficient to induce a 5-fold increase in the number of total ThT$^+$ events when seeded with oligomers whereas no significant generation of new ThT$^+$ species was observed when seeded with sonicated fibrils (Supporting Figure 8A). Again, this points to the likelihood that oligomers are first converting into ThT$^+$ species through a refolding event to become structurally more β-sheet enriched, while fibrils amplify by elongating. Furthermore, seeding experiments with oligomers had an increased proportion of S and H particles within 2.5 h and maintained close to a 1:1 ratio (S/H) throughout the prolonged incubation (Supporting Figure 8B). In contrast, PFFs saw a redistribution of the population toward slower diffusing L and N particles.

To test whether the amplification of α-syn oligomers led to the formation of fibrils, we performed a second round of amplification, resupplementing the reaction with additional α-syn monomers. In these conditions, we observed an increase in the number of L- and N-type particles and a right-shift in the scatter plot upon the second round of amplification, suggesting that the first amplification created fibrillar species (Supporting Figure 9).

Sonicated Preformed Fibrils Amplify More Efficiently than Oligomers. The apparent increase in total ThT fluorescence in the amplification assay is much larger for PFFs than for oligomers. When we calculate the increase in median ThT fluorescence of each particle over time, we found that the fluorescence signal has increased by 30-fold when the reaction was seeded with PFFs while seeding with purified oligomers only resulted in a 3-fold increase in fluorescence over a period of 24 h (Figure 6B). The enhanced efficiency of PFFs to amplify is even more dramatic when comparing the effective concentration of seeds, with PFFs used at 2.6 nM (monomer equivalent) or three-orders of magnitude lower concentration than oligomers (2 μM monomer equivalent).

We titrated the concentration of oligomers in seeding experiments to examine whether a higher α-syn monomer/seed ratio may promote faster elongation. As shown in Figure 7A, almost no ThT$^+$ species were detected after amplification

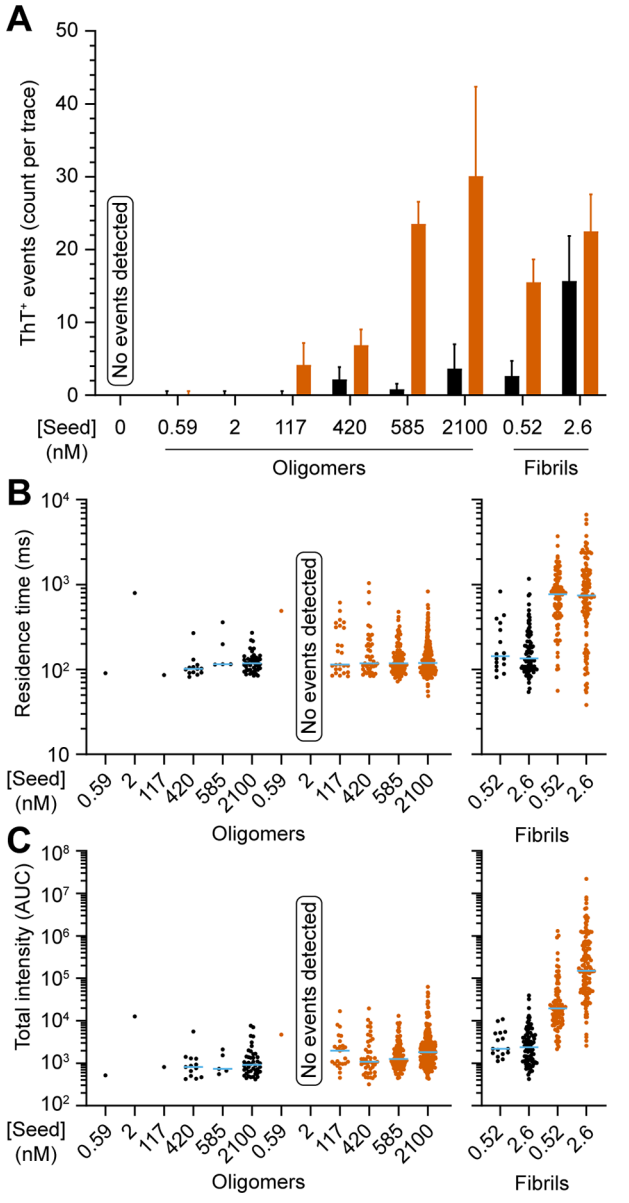

Figure 7. Single molecule amplification assay at different concentration of seeds. (A) Bar graphs showing the number of ThT$^+$ events detected before (black) and after 5 h incubation at 55 °C (red) seeded with oligomers (0.59−2100 nM) and fibrils (0.52 and 2.6 nM). Negative control (no seed) was included. (B) Scatter dot plot of residence time of the ThT$^+$ events detected in panel A showing no change in residence time for oligomers but with significant increase in apparent molecular weight when seeded with fibrils. Blue bar represents median and is omitted when there is <2 data points. Each symbol represents an individual event. (C) Scatter dot plot of total intensity (AUC) for oligomers and PFFs, before (black) and after (red) amplification.

https://doi.org/10.1021/acschemneuro.1c00553
ACS Chem. Neurosci. 2022, 13, 883−896

at <2 nM of oligomers. The lowest seeding concentration of 117 nM of oligomers produced particles with a median residence time that was identical to the one observed in the sample seeded with 2100 nM of oligomers (116 and 119 ms, respectively, Figure 7B). In contrast, seeding at 2.6 nM and 0.52 nM fibrils both resulted with significant increase in apparent diffusion to ∼750 ms in residence time (Figure 7B). Importantly, we observed that changes in overall fluorescence (AUC) is much larger for PFFs than for oligomers at all seeding concentrations tested (Figure 7C).

We also validated that presence of ThT *in situ* during the seeding experiment did not interfere with the ability of oligomers to seed as single molecule results were identical between ThT^+ particles stained *in situ* or after the seeding reaction (see Supporting Results and Supporting Figure 10). ThT does not interfere with the elongation and remodeling of oligomers and improved the seeding efficiency for fibrils. Thus, it appears that oligomers can seed to form small protofibrils but are significantly slower in polymerization compared to mature fibrils. We conclude that fibrils have significantly higher amplification (seeding) potential in comparison to their earlier oligomeric precursors.

Lyophilization of Oligomers. We also examined the seeding potential of oligomers that were lyophilized given that many therapeutic proteins can benefit from long-term storage. We took α-syn oligomers obtained by SEC from two independent batches of α-syn aggregation experiments and lyophilized the frozen oligomers in the same ways that monomers were prepared. The lyophilized oligomers were reconstituted by adding water to restore the original salt concentration (1× PBS) and single molecule amplification was performed to assess their seeding potential compared to those in nonlyophilized state. We observed that the lyophilization process produced significantly more ThT^+ aggregates in the fluorescence traces of non amplified oligomers (Supporting Figure 11). However, the number of ThT^+ species after amplification is identical between the two samples. Non-lyophilized samples produced about 6-fold change in ThT^+ events compared to a 2-fold change for lyophilized oligomers suggesting that the lyophilization produced species may not be seeding competent.

One of the main challenges of performing *in vitro* studies to model Parkinson's disease is the heterogeneity of α-syn preparations, which can have direct consequences on experimental reproducibility. Increasingly, observations that amyloid strains, including in α-syn fibrils, play decisive roles in disease presentation and progression further increase this concern. The notion of "oligomers" itself remains ill-defined and has been used to describe subspecies of different sizes, shapes, and properties of α-syn aggregates depending on the preparation protocol used. For these reasons, a better definition of the subspecies and a standardization of protocols is needed so that data can be more robustly reproduced and compared. Significant efforts in recent years have been directed to standardize or characterize α-syn oligomers or PFFs. Approaches such as electron microscopy, atomic force microscopy, dynamic light scattering, and circular dichroism have been used for the physical characterization of α-syn subspecies while biochemical assessments include proteinase digestion and the examination of aggregation kinetics.[4,5,17,25] Most of these methods perform measurements in bulk and thus do not easily reveal the heterogeneity of the preparations. We have established that the detection limit for PFFs using AttoBright was 1 pM monomer equivalent.[34] Our highly sensitive single molecule method was used here to track the aggregation at different steps and to compare the size and reactivity of the different α-syn species (monomers, oligomers and fibrils). After low-speed centrifugation of a 5 h aggregation reaction (18000*g* for 10 min), many fibrils were still present in the supernatant and dominated the fluorescence time trace (Supporting Figure 2). High speed centrifugation (100000*g* for 30 min) effectively removed large fibrils, but the supernatant profile remained different from the SEC isolated oligomers.[17] Size exclusion chromatography was the preferred approach to obtain oligomers as it excluded both monomeric and fibrillar α-syn. The complete removal of fibrils is important as we propose that minute quantities of fibrils will dominate the signal of oligomers in seed amplification assays.

Here we provided single molecule profiles of the different α-syn subspecies and showed their relative distribution at different steps of their preparation and purification. We first tracked α-syn aggregation kinetics, and observed that self-assembly occurred rapidly, with ThT^+ events detectable as early as 2.5 h into the incubation. Single molecule fingerprinting showed that small ThT^+ species eventually transformed into slower diffusing protofibrils over time, producing a heterogeneous population of ThT^+ amyloids. The resolution to track the evolution of ThT^+ species over time lends support to the α-syn cascade hypothesis where α-syn monomers generate a population of oligomers that subsequently assemble into larger aggregates. The subsequent isolation of oligomers using gel filtration revealed that a fraction of these oligomers was indeed ThT^+. The estimated concentration of ThT reactive oligomers was ∼0.6 nM (5 events per trace, Supporting Figure 8A) by comparison with sonicated PFFs as our standard (19 events per trace at 2.6 nM). This would imply that only <0.03% of α-syn (of 2 μM) was incorporated into ThT^+ oligomers. We subsequently identified another population of α-syn (∼0.06% of 2 μM obtained from SEC) that became ThT reactive upon incubation with additional monomeric α-syn. We believe that these may correspond to dark oligomers that changed conformation to bind to ThT more efficiently. It could also be that these oligomers converted to short soluble protofibrils, thereby reaching the critical size for detection.[21] Overall, the low proportion of seeding competent oligomers suggests that most of the purified oligomers are possibly off-pathway from fibril formation.

Oligomers principally convert to form more fluorescent species (H-type), both during the initial aggregation process and after purification. This increase in ThT fluorescence of individual aggregates likely stems from remodeling or elongation of the aggregate to form protofibrils. Within a limited range, protofibril growth would occur without significantly affecting the residence time of the object but addition of subunits would increase the number of binding interfaces for ThT. This observation was supported by *in silico* simulation revealing that a magnitude increase in fibrillar length would only produce at most 4-fold increase in residence time (Supporting Figure 6). The single molecule fingerprint of sonicated fibrils was similar to that of α-syn oligomers even though the sonicated PFFs were more heterogeneous and often longer than the oligomers (12 ± 2 nm vs 10−120 nm for the α-syn oligomers and sonicated fibrils, respectively). In the final phase of the kinetics, we observed a conversion of species from S/H to L/N types from the addition of new monomers (Supporting Figure 7). This was similar to the amplification

https://doi.org/10.1021/acschemneuro.1c00553
ACS Chem. Neurosci. 2022, 13, 883−896

profile of the sonicated PFFs and differs from the amplification profile of the oligomers. Overall, these data support the recent observations by Ruggeri et al.[35] where the authors concluded that α-syn aggregation proceeds by an initial elongation of oligomers into single-strand protofibrils that then associate as "double-strand cross-section" protofilaments before forming mature fibrils.

Freeze-drying or lyophilization currently represents almost half of the protein therapeutic market due to its considerable enhancement in stability compared to solution state (see review by Butreddy et al.[39]) This solid-state form also allows the proteins to be shipped at room temperature especially when a dry ice shipping option is not available or is costly or unreliable during long transit. We thus explored the influence of lyophilization on the stability of α-syn oligomers and their seeding ability. We observed that the reconstitution of lyophilized α-syn oligomers significantly increases the number of ThT^+ particles, with no apparent change in the final number of amplifiable oligomers (Supporting Figure 11).

The biological implication of toxicity between fibrils and oligomers remains controversial. On one hand, certain types of α-syn oligomers were demonstrated to trigger calcium influx induced cell death in SH-SY5Y cell lines.[25,30] Similarly, the oligomer-forming mutants E35K and E57K have higher affinities to interact with liposomes *in vitro*, and in a rat model of synucleinopathies higher rates of cell death have been reported with these mutations.[4] On the other hand, fibrils are the accumulated species in Lewy bodies that are pathognomonic of PD with higher seeding potential for cell−cell transmission.[40,41] These differing observations emphasize the need to correctly segregate and characterize each species prior to biological experiments. While these *in vitro* and *ex vivo* experiments have provided interesting insights in α-syn aggregation, the biological relevance of α-syn oligomers or fibrils in human biofluids remains an open question. We previously observed that α-syn aggregates amplified from CSF had a specific fingerprint compared to control[34] (albeit in different reaction conditions compared to this study). We hope that further definition of the α-syn species will inform on the biologically relevant assemblies that are found in biofluids.

CONCLUSION

Seed amplification assays (SAAs) are becoming tractable approaches for end-point diagnostic detection due to their high sensitivity to detect α-syn aggregates.[8,9,42,43] However, these tools lack the ability to resolve features that may only be revealed at a single molecule level. The fluorescence approach described here is conceptually equivalent to a SAA since it relies on ThT staining with an amplification step. However, our procedure does not involve mechanical breaking of fibrils, compared to standard SAA.[9] In our hands, sonicated PFFs are far more seeding-competent than α-syn oligomers, at least at early time points of the amplification process. Therefore, it is very likely that the signal observed in SAA will be mainly driven by the presence of fibrils in a sample at low concentration, even if α-syn oligomers were present. Furthermore, we demonstrated that isothermal amplification of sonicated PFFs produced very large species, resulting in a single molecule fingerprint that was distinct from amplified oligomers. Classifying α-syn subspecies based on their biophysical attributes adds an additional layer of granularity in the analysis whereby fingerprinting for different types of synucleinopathies may be obtained. This method of single molecule profiling could be applied to the detection and characterization of other types of amyloids (e.g., tau and prion proteins),[44−47] study of other neurodegenerative diseases, or mechanistic investigation of putative cross-talks between α-syn/amyloid-β[48] and α-syn/tau.[48,49] ThT can fluorescently mark other large macromolecular assemblies such as fibrinogen[50] and DNA,[51] thus emphasizing the importance of the isothermal incubation step with the appropriate monomeric substrate for specific detection of amyloids.

MATERIALS AND METHODS

Expression and Purification of Wild-Type Human α-Syn. The plasmid pT7-7 (Addgene 36046)[52] encoding for the human α-synuclein wild-type (α-syn) was transformed into *E. coli* BL21 Rosetta (DE3, pLysS RARE) for expression in Luria−Bertani medium containing ampicillin (100 μg/mL) and chloramphenicol (34 μg/mL) at 37 °C. Protein expression was induced with isopropyl β-D-1-thiogalactopyranoside (IPTG, 1 mM) at an optical density (600 nm) of 0.5 and allowed to proceed at 18 °C for 16 h with shaking. Cells were harvested with centrifugation, resuspended in cold lysis buffer (25 mM Tris, pH 8, 0.02% w/v NaN_3, Complete protease inhibitor, Roche, 04693132001) and lysed using the CF cell disruptor (Constant Systems Ltd.) at 20000 PSI. Lysate was supplemented with EDTA (10 mM) and incubated at 90 °C for 20 min to precipitate bacterial proteins. Lysate was clarified by centrifugation (Thermo Fisher Scientific, SS-34 rotor, 19000 rpm, 30 min, 4 °C). The supernatant was retained and supplemented with streptomycin sulfate (10 mg/mL, Sigma-Aldrich, S6501-25G), stirred for 20 min at 4 °C and then centrifuged at 19000 rpm (SS-34 rotor, 20 min, 4 °C) to recover the clarified supernatant. These incubation and centrifugation steps were repeated with 20 and 30 mg/mL of streptomycin sulfate. The clarified supernatant was then incubated with ammonium sulfate (0.4 mg/mL) for 30 min at 4 °C and centrifuged at 13600 rpm, 20 min, 4 °C (SS-34). The pellet was resolubilized in buffer A (20 mM Tris, pH 7.7, 0.02% w/v NaN_3) and dialyzed overnight at 4 °C (Thermo Fisher Scientific, 68700). Dialyzed solution was filtered (0.22 μm) and further purified by anion exchange chromatography using 2 HiTrap Capto Q ImpRes columns (Cytiva, 17547055). The column was equilibrated with buffer A before injecting the sample at 1 mL/min. α-Syn eluted at approximately 175 mM NaCl using a linear 300 mL gradient from 0 to 1 M NaCl in buffer A (3 mL/min). Fractions containing α-syn were identified using reducing SDS-PAGE, combined, and concentrated using Amicon Ultra 15 filters (Merck, UFC901024) for size exclusion chromatography. Elution was performed using a HiLoad 16/600 Superdex 200 column (GE Healthcare, 28989335) equilibrated with buffer A at 1 mL/min. Purity was assessed using reducing SDS-PAGE, and samples were concentrated to >343 μM (4.9 mg/mL). Protein concentration was determined spectroscopically at 280 nm absorbance with an extinction coefficient of 5960 M^{-1} cm^{-1}. Purified α-syn was aliquoted, flash frozen with liquid nitrogen, and stored at −80 °C. The yield was 4.2 mg/g of cell mass.

Preparation of α-Syn Oligomers. Generation of α-syn oligomers was based on a protocol by Kumar et al.[17,19] and Rösener et al.[53] Purified α-syn was lyophilized with the LyoQuest freeze-dryer (Telstar) or evaporated at RT with the SpeedVac SC250 (Thermo Fisher Scientific) under vacuum overnight. Tris salts and NaN_3 from buffer A are present in the lyophilized proteins as dialysis was not performed prior to lyophilization. Lyophilized proteins were solubilized in phosphate buffer saline (PBS, 2 mM KH_2PO_4, 10 mM Na_2HPO_4, 2.7 mM KCl and 137 mM NaCl, pH 7.4) to a final α-syn concentration of 12 mg/mL (830 μM) and incubated at 37 °C for 5 h in a vortexer, shaken horizontally at 900 rpm in a 2 mL cryovial. An aliquot of the reaction mixture was withdrawn at different time points for single molecule measurements, flash frozen in liquid nitrogen, and stored at −80 °C until measurement. Approximately 500 μL of aggregation reaction at 5 h was frozen for SEC to purify α-syn oligomers. Five individual α-syn assemblies were performed across

https://doi.org/10.1021/acschemneuro.1c00553
ACS Chem. Neurosci. 2022, 13, 883−896

two different days. Products of the 5 h reactions were thawed at room temperature and centrifuged at 18000*g*, 10 min, 4 °C (Beckman Coulter F301.5 rotor), to remove large aggregates. Pellets were resuspended in PBS and kept for negative staining transmission electron microscopy (EM). The α-syn oligomers and free α-syn monomer from the supernatant were separated using a Superdex 200 Increase 10/300 GL (GE Healthcare, 28990944) equilibrated with PBS. The concentration of α-syn in the different fractions was determined using gel densitometry (see Materials and Methods), and fractions were estimated to contain 0.2−3.1 μM α-syn (monomer equivalent). Afterward, ThT (10 μM) and monomeric α-syn (30 μM) were added to the different fractions, and ThT^+ (ThT reactive) species were measured before and after amplification. Note that the supplementation of α-syn monomer may also minimize the disassembly of oligomers back to monomers after separation[17,54,55] and may prevent binding to the plasticware.[56] Negative controls of monomeric α-syn returned with an average of 1.4 events per trace despite the filtering of the α-syn stock through a 100000 MWCO prior to use (Figure 4A). We believe this low-level detection comes from nonspecific interaction of ThT with reagents trapped in the gel column as similar values were reflected in fractions in the void volume (elution volume 0−7 mL, Figure 4A).

Single Molecule Analysis of Aggregation Kinetics. Aliquots withdrawn at different time points of the oligomer preparation were diluted by 20-fold in PBS containing 10 μM ThT (Sigma-Aldrich, T3516-5G), loaded to a custom polydimethylsiloxane (PDMS) plate adhered to a glass coverslip (ProSciTech, G425-4860) and observed using the inverted 3D printed confocal microscope, "AttoBright", equipped with a 450 nm laser and water immersion 40×/1.2 NA objective (Zeiss).[32] Emitted fluorescence from ThT was filtered by a dichroic mirror (488 nm) and a long-pass filter (500 nm) before focusing onto a single photon avalanche diode (Micro Photon Devices). Fluorescence spectroscopy traces were recorded for 100 s/trace in 10 ms bins and analyzed using a custom python script (see Supporting Information) on Spyder version 4.0.1 to extract information on large intensity bursts (peaks) in the fluorescent traces in an automated and unbiased manner.

The analysis script reports on the following:

1. The prominence of each burst. This represents the intensity of a peak corrected for background fluorescence. The prominence of each peak was determined by extending a horizontal line from the peak maxima to the left and right to intersect the raw signal. The lowest intensity value between the peak maxima and the new intercepts forms the base of a peak. Prominence is then defined as the difference of the lowest of the two intensity values of the bases and the peak maximum intensity.
2. The residence time or the full width at half-maximum (fwhm) of a burst. Equivalently, it is the difference of two time points in which the intensity values are at 50% of the prominence.
3. The total intensity of each fluorescence burst, defined as the sum of intensities between the upper and lower limit of the fwhm to estimate the area under the curve (AUC).

We determined that the fwhm of a peak provided a more reliable metric compared to using 90% of prominence or 100% (full width). This is because the latter gave rise to artificially large residence times, compounded by the fact that a Gaussian peak stretches to infinity in which peak bases can never be defined. Thus, the total intensity currently reported is an underestimation of the true intensity of each burst.

Amplification of α-Syn Oligomers. SEC eluted fractions (in PBS) were mixed with filtered monomeric α-syn WT (30 μM) and ThT (10 μM) and were incubated at 55 or 37 °C for 5 h in a PCR machine (Biorad, C1000) for amplification.[34] Fractions comprised of ≥76% of its original volume were mixed with α-syn monomers and ThT to reach a final volume of 20 μL per reaction. Samples were loaded without dilution onto the PDMS plate to record fluorescence on AttoBright. Fluorescence was recorded in 100 s/trace, 10 ms bins and was analyzed using the custom script as previously described. Fractions that revealed significant positive increase in the number of ThT peaks after amplification were designated as fractions containing α-syn oligomers. These fractions were reproducibly identified across different SEC experiments, and traces were pooled together for analysis.

Production and Sonication of α-Syn Preformed Fibrils. Human α-syn WT preformed fibrils (PFFs) were generated by incubating a solution of monomeric α-syn WT (208 μM) in PBS at 45 °C with shaking (500 rpm) for 72 h in the presence of a ministirrer. The solution was sonicated for 15 min at 12 h then every 24 h at room temperature in a water bath (Ultrasonics, FXP 14M) to induce fragmentation of the fibrils. PFFs were snap frozen in liquid nitrogen and stored at −80 °C for future use. PFFs were thawed, loaded to a Microtube-50 AFA screw capped capsule (Covaris) and sonicated using a Covaris focused ultrasonicator (M220) for 10 min, 5 s on/off at 75 W, 12 °C. Samples were kept in the capsule at RT.

Time Course Amplification of α-Syn Preformed Fibrils and Oligomers. Sonicated PFFs (2.6 nM) and three different elution fractions containing amplifiable oligomers (0.15−2.4 μM α-syn) were mixed with α-syn WT filtered through a 100000 MWCO membrane (30 μM) and ThT (10 μM) in PBS. Reactions were aliquoted for immediate fluorescence measurements on the AttoBright and for measurements after 2.5, 5, 7.5, and 24 h incubation at 55 °C. Fractions seeded with oligomers were pooled during the analysis using the custom peak analysis script.

Negative Staining Transmission Electron Microscopy. A copper grid (200 mesh, coated with carbon and Formvar, Ted Pella, 01811) was cleaned by glow discharged and a small solution of samples, pellet and supernatant of the reaction mixture, oligomeric fractions from SEC, and preformed and sonicated fibrils, were applied onto the grid and wicked dry. The grid was washed with a drop of Milli-Q water and immediately wicked dry to minimize phosphate deposit. This was repeated two more times. The grid was then stained with a drop of uranyl acetate (2% w/v) and wicked dry immediately. This process was repeated twice, and the grid was air-dried. Micrographs were collected using a FEI Tecnai G2 20 electron microscopes at 38000-fold magnification. Particle diameters were measured using ImageJ.

Estimation of Protein Concentration. The concentration α-syn from the purification was estimated spectrophotometrically with extinction coefficient of 5930 M^{-1} cm^{-1} at 280 nm. The protein concentration in SEC eluted fractions was spectroscopically too low for accurate quantification. Therefore, the concentration of α-syn was estimated using gel densitometry with a known amount of α-syn WT (100−3200 ng, determined spectroscopically) loaded on reducing SDS-PAGE as standard. Protein bands were revealed with 1 h staining with SimplyBlue Safe stain (Thermo Fisher Scientific, LC6065) and overnight destaining in water. The gel was imaged using the Chemi-doc system (Biorad) with Cy5.5 filter, which provided a linear readout for interpolation. The concentration of α-syn in the eluted fractions containing oligomers was low, in the range 0.2−3.1 μM.

■ ASSOCIATED CONTENT

Supporting Information

The Supporting Information includes The Supporting Information is available free of charge at https://pubs.acs.org/doi/10.1021/acschemneuro.1c00553.

Supporting materials and methods, single molecule traces of time course aggregation experiments, single molecule profiling of aggregation reaction and supernatant, single molecule profiling of the supernatant collected after a high-speed centrifugation compared to purified oligomers, representative fluorescence traces showing the effects of amplification on oligomers, effect on the seeding potential of oligomers at different temperatures, simulation of the change in apparent diffusion as a function of aspect ratio, seeding of fibrils in the absence of α-syn monomers, distribution of α-syn species in longitudinal study, second round of

https://doi.org/10.1021/acschemneuro.1c00553
ACS Chem. Neurosci. 2022, 13, 883−896

amplification of purified oligomers, effect of ThT in amplification assay, effects of lyophilization on purified oligomers, incubation at physiological temperature to detect ThT species, requirement for α-syn monomers for changes in single molecule profiles, ThT effect on the seeding efficiency of oligomers and fibrils, decrease of seeding potential of oligomers due to lyophilization, and single molecule analysis script (PDF)

AUTHOR INFORMATION

Corresponding Authors

Antony Cooper − *The Australian Parkinson's Mission, The Garvan Institute of Medical Research, Darlinghurst, New South Wales 2010, Australia; St Vincent's Clinical School, UNSW Sydney, Darlinghurst, New South Wales 2010, Australia*; Email: a.cooper@garvan.org.au

Yann Gambin − *EMBL Australia Node for Single Molecule Sciences and School of Medical Sciences, Faculty of Medicine, the University of New South Wales, Sydney, New South Wales 2052, Australia*; Email: y.gambin@unsw.edu.au

Emma Sierecki − *EMBL Australia Node for Single Molecule Sciences and School of Medical Sciences, Faculty of Medicine, the University of New South Wales, Sydney, New South Wales 2052, Australia*; orcid.org/0000-0001-9970-868X; Email: e.sierecki@unsw.edu.au

Authors

Derrick Lau − *EMBL Australia Node for Single Molecule Sciences and School of Medical Sciences, Faculty of Medicine, the University of New South Wales, Sydney, New South Wales 2052, Australia*; orcid.org/0000-0002-9311-647X

Chloé Magnan − *EMBL Australia Node for Single Molecule Sciences and School of Medical Sciences, Faculty of Medicine, the University of New South Wales, Sydney, New South Wales 2052, Australia*

Kathryn Hill − *The Australian Parkinson's Mission, The Garvan Institute of Medical Research, Darlinghurst, New South Wales 2010, Australia*

Complete contact information is available at: https://pubs.acs.org/10.1021/acschemneuro.1c00553

Author Contributions

D.L. performed all the experiments and analyzed data. C.M. wrote the analysis software (Python) and helped analyze data. K.H. prepared reagents and participated in data collection. A.C., Y.G., and E.S. conceptualized and supervised the experiments. All authors participated in writing and editing of the manuscript.

Notes

The authors declare the following competing financial interest(s): Y.G. and E.S. are founders of AttoQuest and inventors of the AttoBright instrument (PCT AU2019/050188).

ACKNOWLEDGMENTS

This work was supported by grant MJFF-010267 from the Michael J Fox Foundation for Parkinson's research and Shake it Up! Australia (to E.S., Y.G., and A.C.). A.C. received grant funding from the Australian Government. The authors thank Richard Morris from the EMBL Australia Single Molecule Science Node at the University of New South Wales for helpful discussion and advice on predicting the changes in residence time as a function of size of rod-like particles.

REFERENCES

(1) Jankovic, J. Parkinson's disease: clinical features and diagnosis. *J. Neurol Neurosurg Psychiatry* **2008**, *79* (4), 368−76.

(2) Baba, M.; Nakajo, S.; Tu, P. H.; Tomita, T.; Nakaya, K.; Lee, V. M.; Trojanowski, J. Q.; Iwatsubo, T. Aggregation of alpha-synuclein in Lewy bodies of sporadic Parkinson's disease and dementia with Lewy bodies. *Am. J. Pathol.* **1998**, *152* (4), 879−84.

(3) Polymeropoulos, M. H.; Lavedan, C.; Leroy, E.; Ide, S. E.; Dehejia, A.; Dutra, A.; Pike, B.; Root, H.; Rubenstein, J.; Boyer, R.; Stenroos, E. S.; Chandrasekharappa, S.; Athanassiadou, A.; Papapetropoulos, T.; Johnson, W. G.; Lazzarini, A. M.; Duvoisin, R. C.; Di Iorio, G.; Golbe, L. I.; Nussbaum, R. L. Mutation in the alpha-synuclein gene identified in families with Parkinson's disease. *Science* **1997**, *276* (5321), 2045−7.

(4) Winner, B.; Jappelli, R.; Maji, S. K.; Desplats, P. A.; Boyer, L.; Aigner, S.; Hetzer, C.; Loher, T.; Vilar, M.; Campioni, S.; Tzitzilonis, C.; Soragni, A.; Jessberger, S.; Mira, H.; Consiglio, A.; Pham, E.; Masliah, E.; Gage, F. H.; Riek, R. In vivo demonstration that alpha-synuclein oligomers are toxic. *Proc. Natl. Acad. Sci. U. S. A.* **2011**, *108* (10), 4194−9.

(5) Lashuel, H. A.; Petre, B. M.; Wall, J.; Simon, M.; Nowak, R. J.; Walz, T.; Lansbury, P. T., Jr. Alpha-synuclein, especially the Parkinson's disease-associated mutants, forms pore-like annular and tubular protofibrils. *J. Mol. Biol.* **2002**, *322* (5), 1089−102.

(6) Konno, T.; Ross, O. A.; Puschmann, A.; Dickson, D. W.; Wszolek, Z. K. Autosomal dominant Parkinson's disease caused by SNCA duplications. *Parkinsonism Relat Disord* **2016**, *22* (Suppl 1), S1−S6.

(7) Spillantini, M. G.; Crowther, R. A.; Jakes, R.; Hasegawa, M.; Goedert, M. alpha-Synuclein in filamentous inclusions of Lewy bodies from Parkinson's disease and dementia with lewy bodies. *Proc. Natl. Acad. Sci. U. S. A.* **1998**, *95* (11), 6469−73.

(8) Shahnawaz, M.; Mukherjee, A.; Pritzkow, S.; Mendez, N.; Rabadia, P.; Liu, X.; Hu, B.; Schmeichel, A.; Singer, W.; Wu, G.; Tsai, A. L.; Shirani, H.; Nilsson, K. P. R.; Low, P. A.; Soto, C. Discriminating α-synuclein strains in Parkinson's disease and multiple system atrophy. *Nature* **2020**, *578* (7794), 273−277.

(9) Rossi, M.; Candelise, N.; Baiardi, S.; Capellari, S.; Giannini, G.; Orrù, C. D.; Antelmi, E.; Mammana, A.; Hughson, A. G.; Calandra-Buonaura, G.; Ladogana, A.; Plazzi, G.; Cortelli, P.; Caughey, B.; Parchi, P. Ultrasensitive RT-QuIC assay with high sensitivity and specificity for Lewy body-associated synucleinopathies. *Acta Neuropathol* **2020**, *140* (1), 49−62.

(10) Russo, M. J.; Orru, C. D.; Concha-Marambio, L.; Giaisi, S.; Groveman, B. R.; Farris, C. M.; Holguin, B.; Hughson, A. G.; LaFontant, D. E.; Caspell-Garcia, C.; Coffey, C. S.; Mollon, J.; Hutten, S. J.; Merchant, K.; Heym, R. G.; Soto, C.; Caughey, B.; Kang, U. J. High diagnostic performance of independent alpha-synuclein seed amplification assays for detection of early Parkinson's disease. *Acta Neuropathol Commun.* **2021**, *9* (1), 179.

(11) Iranzo, A.; Fairfoul, G.; Ayudhaya, A. C. N.; Serradell, M.; Gelpi, E.; Vilaseca, I.; Sanchez-Valle, R.; Gaig, C.; Santamaria, J.; Tolosa, E.; Riha, R. L.; Green, A. J. E. Detection of α-synuclein in CSF by RT-QuIC in patients with isolated rapid-eye-movement sleep behaviour disorder: a longitudinal observational study. *Lancet Neurol* **2021**, *20* (3), 203−212.

(12) Bhattacharjee, P.; Öhrfelt, A.; Lashley, T.; Blennow, K.; Brinkmalm, A.; Zetterberg, H. Mass Spectrometric Analysis of Lewy Body-Enriched α-Synuclein in Parkinson's Disease. *J. Proteome Res.* **2019**, *18* (5), 2109−2120.

(13) Sorrentino, Z. A.; Giasson, B. I. The emerging role of α-synuclein truncation in aggregation and disease. *J. Biol. Chem.* **2020**, *295* (30), 10224−10244.

(14) Fujiwara, H.; Hasegawa, M.; Dohmae, N.; Kawashima, A.; Masliah, E.; Goldberg, M. S.; Shen, J.; Takio, K.; Iwatsubo, T. alpha-

Synuclein is phosphorylated in synucleinopathy lesions. *Nat. Cell Biol.* **2002**, *4* (2), 160−4.
(15) Giasson, B. I.; Duda, J. E.; Murray, I. V.; Chen, Q.; Souza, J. M.; Hurtig, H. I.; Ischiropoulos, H.; Trojanowski, J. Q.; Lee, V. M.-Y. Oxidative damage linked to neurodegeneration by selective alpha-synuclein nitration in synucleinopathy lesions. *Science* **2000**, *290* (5493), 985−9.
(16) Zucchelli, S.; Codrich, M.; Marcuzzi, F.; Pinto, M.; Vilotti, S.; Biagioli, M.; Ferrer, I.; Gustincich, S. TRAF6 promotes atypical ubiquitination of mutant DJ-1 and alpha-synuclein and is localized to Lewy bodies in sporadic Parkinson's disease brains. *Hum. Mol. Genet.* **2010**, *19* (19), 3759−70.
(17) Kumar, S. T.; Donzelli, S.; Chiki, A.; Syed, M. M. K.; Lashuel, H. A. A simple, versatile and robust centrifugation-based filtration protocol for the isolation and quantification of α-synuclein monomers, oligomers and fibrils: Towards improving experimental reproducibility in α-synuclein research. *J. Neurochem* **2020**, *153* (1), 103−119.
(18) Ruesink, H.; Reimer, L.; Gregersen, E.; Moeller, A.; Betzer, C.; Jensen, P. H. Stabilization of α-synuclein oligomers using form-aldehyde. *PLoS One* **2019**, *14* (10), e0216764.
(19) Paslawski, W.; Lorenzen, N.; Otzen, D. E. Formation and Characterization of α-Synuclein Oligomers. *Methods Mol. Biol.* **2016**, *1345*, 133−50.
(20) Rossi, M.; Baiardi, S.; Teunissen, C. E.; Quadalti, C.; van de Beek, M.; Mammana, A.; Stanzani-Maserati, M.; Van der Flier, W. M.; Sambati, L.; Zenesini, C.; Caughey, B.; Capellari, S.; Lemstra, A. W.; Parchi, P. Diagnostic Value of the CSF α-Synuclein Real-Time Quaking-Induced Conversion Assay at the Prodromal MCI Stage of Dementia With Lewy Bodies. *Neurology* **2021**, *97* (9), e930−e940.
(21) Zhou, L.; Kurouski, D. Structural Characterization of Individual α-Synuclein Oligomers Formed at Different Stages of Protein Aggregation by Atomic Force Microscopy-Infrared Spectroscopy. *Anal. Chem.* **2020**, *92* (10), 6806−6810.
(22) Ludtmann, M. H. R.; Angelova, P. R.; Horrocks, M. H.; Choi, M. L.; Rodrigues, M.; Baev, A. Y.; Berezhnov, A. V.; Yao, Z.; Little, D.; Banushi, B.; Al-Menhali, A. S.; Ranasinghe, R. T.; Whiten, D. R.; Yapom, R.; Dolt, K. S.; Devine, M. J.; Gissen, P.; Kunath, T.; Jaganjac, M.; Pavlov, E. V.; Klenerman, D.; Abramov, A. Y.; Gandhi, S. α-synuclein oligomers interact with ATP synthase and open the permeability transition pore in Parkinson's disease. *Nat. Commun.* **2018**, *9* (1), 2293.
(23) Mazzulli, J. R.; Xu, Y. H.; Sun, Y.; Knight, A. L.; McLean, P. J.; Caldwell, G. A.; Sidransky, E.; Grabowski, G. A.; Krainc, D. Gaucher disease glucocerebrosidase and α-synuclein form a bidirectional pathogenic loop in synucleinopathies. *Cell* **2011**, *146* (1), 37−52.
(24) Yap, T. L.; Velayati, A.; Sidransky, E.; Lee, J. C. Membrane-bound α-synuclein interacts with glucocerebrosidase and inhibits enzyme activity. *Mol. Genet. Metab.* **2013**, *108* (1), 56−64.
(25) Danzer, K. M.; Haasen, D.; Karow, A. R.; Moussaud, S.; Habeck, M.; Giese, A.; Kretzschmar, H.; Hengerer, B.; Kostka, M. Different species of alpha-synuclein oligomers induce calcium influx and seeding. *J. Neurosci.* **2007**, *27* (34), 9220−32.
(26) Emmanouilidou, E.; Stefanis, L.; Vekrellis, K. Cell-produced alpha-synuclein oligomers are targeted to, and impair, the 26S proteasome. *Neurobiol Aging* **2010**, *31* (6), 953−68.
(27) Gonçalves, S. A.; Outeiro, T. F. Traffic jams and the complex role of α-Synuclein aggregation in Parkinson disease. *Small GTPases* **2017**, *8* (2), 78−84.
(28) Mahul-Mellier, A. L.; Burtscher, J.; Maharjan, N.; Weerens, L.; Croisier, M.; Kuttler, F.; Leleu, M.; Knott, G. W.; Lashuel, H. A. The process of Lewy body formation, rather than simply α-synuclein fibrillization, is one of the major drivers of neurodegeneration. *Proc. Natl. Acad. Sci. U. S. A.* **2020**, *117* (9), 4971−4982.
(29) Skamris, T.; Marasini, C.; Madsen, K. L.; Foderà, V.; Vestergaard, B. Early Stage Alpha-Synuclein Amyloid Fibrils are Reservoirs of Membrane-Binding Species. *Sci. Rep.* **2019**, *9* (1), 1733.
(30) Cascella, R.; Chen, S. W.; Bigi, A.; Camino, J. D.; Xu, C. K.; Dobson, C. M.; Chiti, F.; Cremades, N.; Cecchi, C. The release of toxic oligomers from α-synuclein fibrils induces dysfunction in neuronal cells. *Nat. Commun.* **2021**, *12* (1), 1814.
(31) Priest, D. G.; Solano, A.; Lou, J.; Hinde, E. Fluorescence fluctuation spectroscopy: an invaluable microscopy tool for uncovering the biophysical rules for navigating the nuclear landscape. *Biochem. Soc. Trans.* **2019**, *47* (4), 1117−1129.
(32) Brown, J. W. P.; Bauer, A.; Polinkovsky, M. E.; Bhumkar, A.; Hunter, D. J. B.; Gaus, K.; Sierecki, E.; Gambin, Y. Single-molecule detection on a portable 3D-printed microscope. *Nat. Commun.* **2019**, *10* (1), 5662.
(33) Naiki, H.; Higuchi, K.; Hosokawa, M.; Takeda, T. Fluorometric determination of amyloid fibrils in vitro using the fluorescent dye, thioflavin T1. *Anal. Biochem.* **1989**, *177* (2), 244−9.
(34) Bhumkar, A.; Magnan, C.; Lau, D.; Jun, E. S. W.; Dzamko, N.; Gambin, Y.; Sierecki, E. Single-Molecule Counting Coupled to Rapid Amplification Enables Detection of α-Synuclein Aggregates in Cerebrospinal Fluid of Parkinson's Disease Patients. *Angew. Chem., Int. Ed. Engl.* **2021**, *133*, 11981.
(35) Ruggeri, F. S.; Benedetti, F.; Knowles, T. P. J.; Lashuel, H. A.; Sekatskii, S.; Dietler, G. Identification and nanomechanical characterization of the fundamental single-strand protofilaments of amyloid α-synuclein fibrils. *Proc. Natl. Acad. Sci. U. S. A.* **2018**, *115* (28), 7230−7235.
(36) Mehra, S.; Sahay, S.; Maji, S. K. α-Synuclein misfolding and aggregation: Implications in Parkinson's disease pathogenesis. *Biochim Biophys Acta Proteins Proteomics* **2019**, *1867* (10), 890−908.
(37) Pieri, L.; Madiona, K.; Melki, R. Structural and functional properties of prefibrillar α-synuclein oligomers. *Sci. Rep* **2016**, *6*, 24526.
(38) Bousset, L.; Pieri, L.; Ruiz-Arlandis, G.; Gath, J.; Jensen, P. H.; Habenstein, B.; Madiona, K.; Olieric, V.; Böckmann, A.; Meier, B. H.; Melki, R. Structural and functional characterization of two alpha-synuclein strains. *Nat. Commun.* **2013**, *4*, 2575.
(39) Butreddy, A.; Janga, K. Y.; Ajjarapu, S.; Sarabu, S.; Dudhipala, N. Instability of therapeutic proteins - An overview of stresses, stabilization mechanisms and analytical techniques involved in lyophilized proteins. *Int. J. Biol. Macromol.* **2021**, *167*, 309−325.
(40) Hansen, C.; Angot, E.; Bergström, A. L.; Steiner, J. A.; Pieri, L.; Paul, G.; Outeiro, T. F.; Melki, R.; Kallunki, P.; Fog, K.; Li, J. Y.; Brundin, P. α-Synuclein propagates from mouse brain to grafted dopaminergic neurons and seeds aggregation in cultured human cells. *J. Clin Invest* **2011**, *121* (2), 715−25.
(41) Luk, K. C.; Song, C.; O'Brien, P.; Stieber, A.; Branch, J. R.; Brunden, K. R.; Trojanowski, J. Q.; Lee, V. M. Exogenous alpha-synuclein fibrils seed the formation of Lewy body-like intracellular inclusions in cultured cells. *Proc. Natl. Acad. Sci. U. S. A.* **2009**, *106* (47), 20051−6.
(42) Sano, K.; Atarashi, R.; Satoh, K.; Ishibashi, D.; Nakagaki, T.; Iwasaki, Y.; Yoshida, M.; Murayama, S.; Mishima, K.; Nishida, N. Prion-Like Seeding of Misfolded α-Synuclein in the Brains of Dementia with Lewy Body Patients in RT-QUIC. *Mol. Neurobiol* **2018**, *55* (5), 3916−3930.
(43) Singh, S.; DeMarco, M. L. In Vitro Conversion Assays Diagnostic for Neurodegenerative Proteinopathies. *J. Appl. Lab Med.* **2020**, *5* (1), 142−157.
(44) Kraus, A.; Saijo, E.; Metrick, M. A., 2nd; Newell, K.; Sigurdson, C. J.; Zanusso, G.; Ghetti, B.; Caughey, B. Seeding selectivity and ultrasensitive detection of tau aggregate conformers of Alzheimer disease. *Acta Neuropathol* **2019**, *137* (4), 585−598.
(45) Fiorini, M.; Iselle, G.; Perra, D.; Bongianni, M.; Capaldi, S.; Sacchetto, L.; Ferrari, S.; Mombello, A.; Vascellari, S.; Testi, S.; Monaco, S.; Zanusso, G. High Diagnostic Accuracy of RT-QuIC Assay in a Prospective Study of Patients with Suspected sCJD. *Int. J. Mol. Sci.* **2020**, *21* (3), 880.
(46) Ray, S.; Singh, N.; Kumar, R.; Patel, K.; Pandey, S.; Datta, D.; Mahato, J.; Panigrahi, R.; Navalkar, A.; Mehra, S.; Gadhe, L.; Chatterjee, D.; Sawner, A. S.; Maiti, S.; Bhatia, S.; Gerez, J. A.; Chowdhury, A.; Kumar, A.; Padinhateeri, R.; Riek, R.; Krishnamoorthy, G.; Maji, S. K. α-Synuclein aggregation nucleates

through liquid-liquid phase separation. *Nat. Chem.* **2020**, *12* (8), 705−716.
(47) Whiten, D. R.; Cox, D.; Horrocks, M. H.; Taylor, C. G.; De, S.; Flagmeier, P.; Tosatto, L.; Kumita, J. R.; Ecroyd, H.; Dobson, C. M.; Klenerman, D.; Wilson, M. R. Single-Molecule Characterization of the Interactions between Extracellular Chaperones and Toxic α-Synuclein Oligomers. *Cell Rep* **2018**, *23* (12), 3492−3500.
(48) Kayed, R.; Dettmer, U.; Lesné, S. E. Soluble endogenous oligomeric α-synuclein species in neurodegenerative diseases: Expression, spreading, and cross-talk. *J. Parkinsons Dis* **2020**, *10* (3), 791−818.
(49) Castillo-Carranza, D. L.; Guerrero-Muñoz, M. J.; Sengupta, U.; Gerson, J. E.; Kayed, R. α-Synuclein Oligomers Induce a Unique Toxic Tau Strain. *Biol. Psychiatry* **2018**, *84* (7), 499−508.
(50) Talens, S.; Leebeek, F. W. G.; Veerhuis, R.; Rijken, D. C. Decoration of Fibrin with Extracellular Chaperones. *Thromb Haemost* **2019**, *119* (10), 1624−1631.
(51) Biancardi, A.; Biver, T.; Burgalassi, A.; Mattonai, M.; Secco, F.; Venturini, M. Mechanistic aspects of thioflavin-T self-aggregation and DNA binding: evidence for dimer attack on DNA grooves. *Phys. Chem. Chem. Phys.* **2014**, *16* (37), 20061−72.
(52) Paleologou, K. E.; Schmid, A. W.; Rospigliosi, C. C.; Kim, H. Y.; Lamberto, G. R.; Fredenburg, R. A.; Lansbury, P. T., Jr.; Fernandez, C. O.; Eliezer, D.; Zweckstetter, M.; Lashuel, H. A. Phosphorylation at Ser-129 but not the phosphomimics S129E/D inhibits the fibrillation of alpha-synuclein. *J. Biol. Chem.* **2008**, *283* (24), 16895−905.
(53) Rösener, N. S.; Gremer, L.; Wördehoff, M. M.; Kupreichyk, T.; Etzkorn, M.; Neudecker, P.; Hoyer, W. Clustering of human prion protein and α-synuclein oligomers requires the prion protein N-terminus. *Commun. Biol.* **2020**, *3* (1), 365.
(54) Du, X. Y.; Xie, X. X.; Liu, R. T. The Role of α-Synuclein Oligomers in Parkinson's Disease. *Int. J. Mol. Sci.* **2020**, *21* (22), 8645.
(55) Roberts, H. L.; Brown, D. R. Seeking a mechanism for the toxicity of oligomeric α-synuclein. *Biomolecules* **2015**, *5* (2), 282−305.
(56) Bousset, L.; Brundin, P.; Böckmann, A.; Meier, B.; Melki, R. An Efficient Procedure for Removal and Inactivation of Alpha-Synuclein Assemblies from Laboratory Materials. *J. Parkinsons Dis* **2016**, *6* (1), 143−51.

https://doi.org/10.1021/acschemneuro.1c00553
ACS Chem. Neurosci. 2022, 13, 883−896